https://dx.doi.org/10.1016/j.foodchem.2023.135647

A novel ESKAPE-sensitive peptide with enhanced stability and its application in controlling multiple bacterial contaminations in chilled fresh pork

Ping Zeng [a,b], Pengfei Zhang [a], Lanhua Yi [c,d], Kwok-Yin Wong [b], Sheng Chen [c], Kin-Fai Chan [b,*], Sharon Shui Yee Leung [a,*]

[a] School of Pharmacy, Faculty of Medicine, The Chinese University of Hong Kong, Shatin, Hong Kong;

[b] State Key Laboratory of Chemical Biology and Drug Discovery and Department of Applied Biology and Chemical Technology, The Hong Kong Polytechnic University, Hung Hom, Kowloon, Hong Kong;

[c] Department of Infectious Diseases and Public Health, Jockey Club College of Veterinary Medicine and Life Sciences, City University of Hong Kong, Kowloon, Hong Kong;

[d] College of Food Science, Southwest University, Chongqing, PR China.

* Corresponding authors

For Kin-Fai Chan, E-mail: kf.chan@polyu.edu.hk

For Sharon Shui Yee Leung, E-mail: sharon.leung@cuhk.edu.hk

Abstract

The co-existence of various pathogenic bacteria on the surface of food products for human consumption greatly aggravated the difficulty of food safety control. Six kinds of highly virulent strains of ESKAPE have been detected in raw or undercooked foods, leading to potentially life-threatening food poisoning worldwide. Due to the increasing prevalence of drug-resistant bacteria, there is an unmet need for the development of food preservatives. In this study, we discovered a novel linear peptide $(IIrr)_4$-NH_2 (**zp80r**) with a broad antibacterial spectrum against all ESKAPE strains and low cytotoxicity to human normal gastric cells. Introducing unnatural amino acid D-arginine dramatically enhanced the proteolytic stability of **zp80r** compared to its natural amino acid L-arginine analog $(IIRR)_4$-NH_2 (**zp80**). Moreover, **zp80r** maintained favourable bioactivities against starvation-induced persisters. Mechanistic studies revealed that **zp80r** killed pathogens by destabilizing cellular envelope structure, causing membrane potential dissipation, pore formation, and cytoplasmic content leakage. Importantly, **zp80r** was able to control multiple bacterial contaminations in chilled fresh pork with improved efficiency in comparison with a known peptide nisin, a bacteriocin that is mainly used in meat products. This newly designed peptide could be a potential antibacterial candidate to combat problematic foodborne pathogens, especially in scenarios with multiple bacteria colonization.

Keywords

helical peptide, broad-spectrum antibacterial, proteolytic stability, membrane targeting, food preservative.

1. Introduction

The ESKAPE pathogens consist of six classes of highly virulent bacteria including - *Enterococcus faecium* (EF), *Staphylococcus aureus* (SA), *Klebsiella pneumoniae* (KP), *Acinetobacter baumannii* (AB), *Pseudomonas aeruginosa* (PA), and *Enterobacter* species [1]. These pathogenic bacteria can literally 'escape' from commonly used antibiotics due to their increasing antibiotic multidrug resistance, posing serious threats to human wellness [2]. Their mechanisms of multidrug resistance include antimicrobial inactivation, biofilm formation, target site modification, and reduction of drug accumulation [3]. A dwindling arsenal of antibiotics has been compelling us to repurpose approved drugs for their possible antibacterial potential, and in the meanwhile, to develop novel molecules with new targets and mechanisms [4].

Consuming contaminated food is a major reason why people infect with morbigenous microorganisms, leading to a large number of foodborne illnesses and heavy economic burdens to society [5]. Among the ESKAPE, EF, SA, PA, and *Enterobacter* species like *Escherichia coli* (EC) O157:H7 and *Enterobacter cloacae* (ECL) were typical foodborne pathogens. KP and AB, which mainly result in respiratory-associated nosocomial infection, were also found in uncooked meat and vegetables [6]. Therefore, the prevention of ESKAPE strains should be an indispensable part of food safety control.

As to the most commonly used commercial food preservatives, benzoate and sorbate salts have advantages like low cost, excellent bioactivity, and negligible acute toxicity [7]. However, their potential hazards, such as cumulative poisoning and human metabolism disruption, have been increasingly concerned in recent years [8]. Rising food safety standards and consumers' preferences have turned the spotlight on novel amino acid-based antibacterial candidates, like bacteriocins, lysins, and protein hydrolysates [9]. Compared with the aforementioned biomacromolecules, linear peptides have unique merits. These peptides possess simple structures that can be easily synthesized by standard solid-phase peptide synthesis (SPPS) [10]. Furthermore, their membrane-targeting nature makes it difficult for pathogens to acquire resistance, particularly important in the post-antibiotic era [11]. Several peptides have been reported for controlling foodborne bacteria such as *Salmonella* [12], *Vibrio* [13], enterohemorrhagic EC (EHEC) [14], and SA [15]. These natural or engineered peptides with promising antibacterial activity provide us with alternative tools to combat notorious microorganisms.

Nevertheless, many peptides demonstrated a limited antibacterial spectrum, reducing their application efficiency when facing multiple bacterial contaminations [16]. ESKAPE consists of two Gram-positive (G+ve) EF, SA and four Gram-negative (G−ve) KP, AB, PA, *Enterobacter* species strains. Different cellular characteristics complicate the situation to discover new food preservatives that show bioactivity against all of them [17]. Therefore, designing a peptide with a broader antibacterial spectrum may contribute to safety control in food products that suffered from simultaneous contaminations by two or more bacterial species [18].

Our previous study investigated an engineered peptide **zp80**, which was able to inhibit the growth of several foodborne pathogens [19]. Its amino acid sequence $(IIRR)_4$-NH_2 was inspired by a classical $(XXYY)_n$-type amphiphilic motif, in which X represented hydrophobic residue,

Y represented hydrophilic residue and n is the number of motifs [20]. However, this hexadecapeptide exhibited relatively weak proteolytic stability in fetal bovine serum (FBS), hindering subsequent development as a highly effective food preservative. In this work, a novel peptide $(IIrr)_4$-NH_2 (**zp80r**) was designed and tested, in which the L-arginines were substituted with the corresponding enantiomers D-arginines. This novel peptide was proved to have improved stability and favorable bioactivities against all ESKAPE strains. Its mode of action and application in controlling multiple bacterial contaminations in chilled fresh pork were evaluated systematically. This study pave the way for the development of novel peptides as food preservatives.

2. Materials and methods

2.1 Peptide synthesis and structural analysis

2.1.1 Peptide synthesis and structural prediction

Peptide **zp80r** was customized by Synpeptide Co., Ltd (Nanjing, China) via SPPS. The crude product was purified by using high-performance liquid chromatography (HPLC) to >98% purity with a linear gradient elution system (gradient: 5 - 95% B in 6 min, flow: 1 mL/min, eluent A: 100% water + 0.05% trifluoroacetic acid; eluent B: 100% acetonitrile + 0.05% trifluoroacetic acid) and a C18 reversed-phase column at detection of 220 nm. The stereo model of **zp80r** was predicted by platform PEPstrMOD (https://webs.iiitd.edu.in/raghava/pepstrmod/) [21]. The amino acid sequence of peptide **zp80** was input into the server. All L-arginines were modified to D-arginines and all L-isoleucines remained unchanged. The amino acid sequence of peptide zp80r was then submitted for structural prediction without changing the advanced options. The obtained stereo model of **zp80r** was downloaded and visualized using the ICM-Browser.

2.1.2 Circular dichroism (CD) spectroscopy

Peptide **zp80r** stock solution (1 mM) was diluted to 0.05 mM by 10 mM sodium dodecyl sulfonate (SDS) solution in deionized water. Signals from 260 nm to 190 nm wavelengths were measured by a J-1500 CD spectrometer (Jasco, Japan). After deducting the background noise (10 mM SDS only), the original data $[\theta]_{obs}$ was converted to $[\theta]$ by the formula $[\theta] = [\theta]_{obs} / 10rlc$. ($[\theta]$ - mean residue ellipticity; r - number of amino acid residue; l - optical path of the sample cell; c - the actual testing concentration of **zp80r**)

2.2 Antibacterial activity and stability analysis

2.2.1 Bacterial strains

Bacterial strains are from our in-house stock. Names with ATCC or BCRC indicate that corresponding strains were standard strains purchased from American Type Culture Collection (USA) or Bioresource Collection and Research Center (Taiwan). Other strains were clinical isolates.

2.2.2 Minimum inhibitory concentration (MIC)

MIC values were determined by broth double dilution method following the guideline of *Methods for dilution antimicrobial susceptibility tests for bacteria that grow aerobically* [22]. Briefly, tested bacteria in the logarithmic phase were diluted to 600 nm optical density (OD_{600}) value at 0.1. Then, a total of 5 μL cell suspension was mixed with 150 μL of Mueller Hinton broth (MHB) medium containing peptide **zp80r** at various concentrations. After 18 hours of incubation at 37°C, the lowest concentration where no observed bacterial growth was defined as the MIC value.

2.2.3 Cleavage sites prediction

Cleavage sites of **zp80** after trypsin treatment were predicted by the Peptide Cutter program in Expasy (https://web.expasy.org/peptide_cutter/) [23].

2.2.4 Peptide degradation degree

Peptide **zp80** and **zp80r** solutions (200 μM) were treated with 4 μg/mL trypsin at 37°C. The samples were analyzed by using HPLC at two hours intervals. The degradation degree was calculated by the ratio of the integral area of the treated group and the untreated group.

2.2.5 MIC in the presence of trypsin

This experiment was performed following the MIC determination protocol mentioned in section 2.2.2 in the presence of trypsin from 0.03 - 4 μg/mL.

2.2.6 MIC in the presence of serum

This experiment was performed following the MIC determination protocol mentioned in section 2.2.2 in the presence of serum concentrations from 0 - 90%.

*2.3 Bioactivities of **zp80r** in various situations*

2.3.1 Persister sensitivity

Cells of EF ATCC49225, SA ATCC29213, PA ATCC15692, and EHEC O157:H7 ATCC43888 in the logarithmic phase were collected and divided into two tubes. One was resuspended in 0.9% NaCl and placed in a constant shaker for 48 hours of incubation at 37°C. The other was resuspended in nutrient broth and placed in a 4°C refrigerator for 48 hours. Then, MIC values were determined following the protocol mentioned in section 2.2.2.

2.3.2 Swarming

Sterile double-layer semisolid plates were fabricated in advance. The bottom layer was normal nutrient agar. After the bottom layer solidifies, 0.5% pure agar containing 10 μM **zp80r** was poured to cover the bottom agar. The ratio of the two layers was 7:3 (bottom: top). Then, 10 μL bacterial solution of EF 188903(2), MRSA ATCC1717, PA MDR-1, and EHEC O157:H7 ATCC43888 (OD_{600} at 0.1) was dropped on the center of the semisolid plate. 24 hours later, swarming pictures were taken by ChemiDoc Imager (Bio-Rad, USA). The longest straight line distance through the center was determined as the motility diameter. The groups without the addition of peptide **zp80r** were set as controls.

2.3.3 Antibacterial efficiency under varied pH values

MHB medium was adjusted to pH at 5 - 9 respectively by HCl or NaOH. Cells of EF 188903(2), MRSA ATCC1717, PA MDR-1, and EHEC O157:H7 ATCC43888 in the logarithmic phase were diluted to their respective OD_{600} at 0.1. For the G+ve group, EF and SA solutions were mixed at the ratio of 1:1. For the G−ve group, PA and EC solutions were mixed at the ratio of 1:1. For the G+ve & G−ve group, four solutions were mixed at the ratio of 1:1:1:1. A total of 5 μL prepared samples were pipetted to a well containing 150 μL MHB medium and peptide **zp80r** at various concentrations. After 24 hours of incubation at 37°C, OD_{600} values for each well were measured by a microplate reader (BMG Clariostar, Germany).

2.3.4 Cytotoxicity

Human gastric epithelial cells (GES-1) were seeded in a 96-well plate in advance. After overnight incubation, **zp80r** at various concentrations was applied to treat them for 24 hours. Then, 3-(4,5-dimethylthiazol-2-yl)-2,5-diphenyltetrazolium bromide (MTT, 20 μL, 5 mg/mL) was added for another 4 hours of staining. After that, the supernatant was removed and a total of 150 μL of dimethylsulfoxide (DMSO) was used to thoroughly dissolve precipitated formazan. Subsequently, 570 nm absorbance values were measured by a microplate reader (BMG Clariostar, Germany). The test group treated with phosphate-buffered saline (PBS) was

defined as 100% survival. The survival ratio of **zp80r**-treated groups was calculated according to the ratio of absorbance value of the peptide-treated versus PBS-treated group. Three biological replicates were performed.

2.4 Action mode

2.4.1 Scanning electron microscopy (SEM)

Cells of EF 188903(2), MRSA ATCC1717, PA MDR-1, and EHEC O157:H7 ATCC43888 in the logarithmic phase were collected and resuspended in sterile PBS until OD_{600} reached 0.6. Then, **zp80r** was added to treat them for 4 hours at their respective 4 MIC at 37°C. Afterward, cells were fixed with 2.5% glutaraldehyde overnight at 4°C. Fixed samples were dehydrated by a graded ethanol series (50, 70, 90, and 100%). Lastly, a volume of 2 μL suspension was dropped onto a clear coverslip. After air drying, and metal coating, cells were imaged by a Quanta 400F field emission SEM (Philips, Netherlands).

2.4.2 Green fluorescent protein (GFP) leakage

GFP-expressing *E. coli* was from an in-house bacterial library. Cells in the logarithmic phase were subjected to 8 μM, 16 μM, and 32 μM **zp80r** treatment respectively. At intervals, cells were rinsed with PBS thrice to remove leaked GFP. Fluorescence units were recorded with an exciting wavelength at 488 nm and an emission wavelength at 525 nm (BMG Clariostar, Germany). Cells without **zp80r** treatment were defined as the controls (GFP 100%).

2.4.3 Confocal image

GFP-expressing *E. coli* cells were treated with PBS and 32 μM **zp80r** respectively for 2 hours. Then, cells were rinsed with PBS thrice to remove leaked GFP. After that, cells were fixed by 2.5% glutaraldehyde for 20 minutes. A total of 2 μL fixed samples were dropped onto a coverslip. Fluorescent images were thus taken by a confocal microscope (Leica TCS SPE, Germany).

2.4.4 Reactive Oxygen Species (ROS)

Bacterial cells of EF 188903(2), MRSA ATCC1717, PA MDR-1, and EHEC O157:H7 ATCC43888 in the logarithmic phase were resuspended in PBS to reach an OD_{600} at 0.6. The cells were divided into five groups and treated with 0.5 MIC, 1 MIC, 2 MIC, 4 MIC **zp80r,** and PBS as control respectively for 1 hour at 37°C. Next, cells were collected and resuspended in PBS containing 10 μM 2,7-dichlorodi-hydrofluorescein diacetate (DCFH-DA) for 30

minutes incubation. After staining, cells were rinsed thrice and their fluorescence units were recorded with an exciting wavelength at 488 nm and an emission wavelength at 525 nm (BMG Clariostar, Germany).

2.4.5 Outer membrane permeability

Final concentrations of 1 MIC and 4 MIC **zp80r** were applied to treat PA MDR-1 and EHEC O157:H7 ATCC43888 cells for 1 hour. Then, 10 μM 1-*N*-phenylnaphthylamine (NPN) was incubated with tested bacterial suspensions. Subsequently, fluorescence units were recorded with an exciting wavelength at 350 nm and an emission wavelength at 420 nm (BMG Clariostar, Germany). The group without **zp80r** treatment was set as the negative control and the group treated with 0.1% Triton X-100 was set as the positive control.

2.4.6 Cytoplasmic membrane permeability

Final concentrations of 1 MIC and 4 MIC **zp80r** were applied to treat EF 188903(2), MRSA ATCC1717, PA MDR-1, and EHEC O157:H7 ATCC43888 cells for 1 hour. Then, 10 μg/mL propidium iodide (PI) was incubated with bacterial suspensions for another 20 minutes. Fluorescence units were recorded with an exciting wavelength at 535 nm and an emission wavelength at 615 nm (BMG Clariostar, Germany). The group without **zp80r** treatment was set as the negative control and the group treated with 0.1% Triton X-100 was set as the positive control.

2.4.7 Membrane potential

Bacterial cells of EF 188903(2) and MRSA ATCC1717 in the logarithmic phase were adjusted to OD_{600} at 0.1 in PBS. Then, cells were treated with 0.5 μM $DiSC_3(5)$ for 1 hour. After rinse and resuspension, **zp80r** at various concentrations were added. Fluorescence units were recorded immediately every 15 seconds with an exciting wavelength at 622 nm and an emission wavelength at 670 nm, lasting for 8 minutes by a microplate reader (BMG Clariostar, Germany).

*2.5 Effect of **zp80r** on pork storage*

2.5.1 Pork spoilage

Chilled fresh pork was purchased from a local market in Hong Kong. It was chopped into small pieces (3 ± 0.2 g) and immersed into mixed bacterial suspension (EF : SA : PA : EC = 1 : 1 : 1 : 1, OD_{600} at 0.5) for 15 minutes of contamination. Thereafter, pork pieces were

immersed in PBS, 4 μM **zp80r**, 16 μM **zp80r**, 64 μM **zp80r,** and 64 μM nisin solutions for 2 hours respectively. Next, they were transferred to a 4°C refrigerator for cold storage. On day 1, day 4, and day 7, pork pieces were brought out to observe the spoilage condition.

2.5.2 Live bacteria counting

After 24 hours of cold storage, the abovementioned contaminated pork pieces were transferred to tubes containing 2 mL PBS. Then, the mixtures vigorously oscillated for 10 minutes. After that, the total live bacteria number was counted based on the method in section 2.6.

2.5.3 SEM for multiple bacterial contaminations

The abovementioned contaminated pork pieces were immersed into PBS solutions containing 0 μM, 4 μM, 16 μM and 32 μM **zp80r** respectively for 4 hours of treatment. Next, pork pieces were removed and bacterial cells were centrifugated. Collected pellets were fixed with 2.5% glutaraldehyde overnight at 4°C. Then, samples were prepared as section 2.14 stated and imaged by a Quanta 400F field emission SEM (Philips, Netherlands).

2.6 Statistical analysis

At least three biological replicates were performed for all experiments. The results were expressed as mean ± standard error. Data analysis was performed by ANOVA and t-tests. In all analyses, $p < 0.05$ was considered significant.

3. Results and discussion

*3.1 Peptide synthesis, quality control, and secondary structure of **zp80r***

Peptide **zp80r** has eight unnatural D-arginine residues, which were highlighted in red in **Figure 1A**. It was easily accessible via standard SPPS at a relatively low cost. The crude product was purified to >98% purity by HPLC. The theoretical molecular weight of **zp80r** is 2171.8105 Da. From the mass spectrum, peaks at 725.0541 Da and 543.9539 Da can be found, indicating the fragments of $[M+3H]^{3+}$ and $[M+4H]^{4+}$ respectively (**Figure 1B**). These results confirmed the successful synthesis of **zp80r** and its >98% purity was sufficient to support subsequent biological evaluation.

In silico structural prediction suggested that **zp80r** presented a helical structure with a clear hydrophilic-hydrophobic interface (**Figure 1C**). This conformation is beneficial both for the molecule to maintain good water solubility and for interaction with the bacterial lipid-rich

membrane surface [24]. The predicted structure of **zp80r** provided an intuitive perspective to observe the distribution of hydrophilic D-arginine and hydrophobic isoleucine residues. Unlike the alternate arrangement of D-arginines and isoleucine in chemical structure, most D-arginine residues were predicted to aggregate on one side and isoleucine residues on another side after the free fold of **zp80r**. This kind of cationic surfactant-like peptide was considered to be a highly-effective cell membrane destroyer [25]. CD spectrum (**Figure 1D**) also confirmed experimentally that **zp80r** could form α-helix structure in an amphiphilic environment.

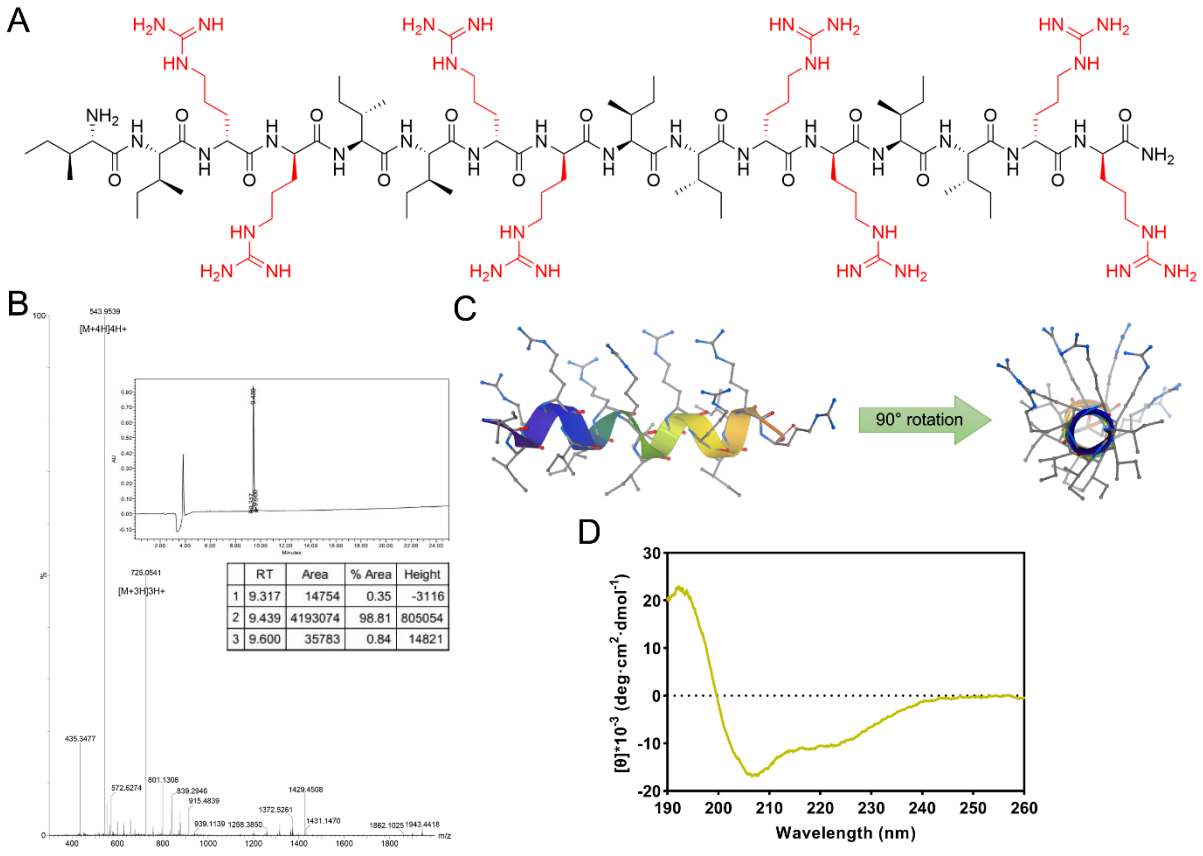

Figure 1. (A) Chemical structure of **zp80r**, D-Arg residues were highlighted in red; (B) Mass and HPLC spectra of **zp80r**; (C) *In silico* structural prediction of **zp80r**; (D) CD spectrum of **zp80r** in 10 mM SDS solution.

*3.2 Peptide **zp80r** has a broad antibacterial spectrum and improved proteolytic stability*

Due to abundant positive charges and meanwhile having hydrophobic moieties, cationic amphiphilic peptides naturally exhibit good affinity with negative-charged phospholipid

bilayers of bacterial cells [26]. This feature may endow them with the ability to physically attack both G+ve and G−ve bacteria indiscriminately, thus presenting a broad antibacterial spectrum [27]. Here, we first determined **zp80r**'s bioactivities against ESKAPE. As illustrated in **Figure 2A**, MIC values of **zp80r** to all tested strains ranged from 1-8 μM, suggesting that **zp80r** was able to prevent ESKAPE from proliferation at the micromole level. Moreover, various superbugs, like methicillin-resistant *Staphylococcus aureus* (MRSA), metallo-beta-lactamase-1 (NDM-1) harbouring PA, *Enterobacter* species, and clinical-isolated carbapenem-resistant KP, were sensitive to **zp80r**. These data proved **zp80r**'s antibacterial potency and wide applicability.

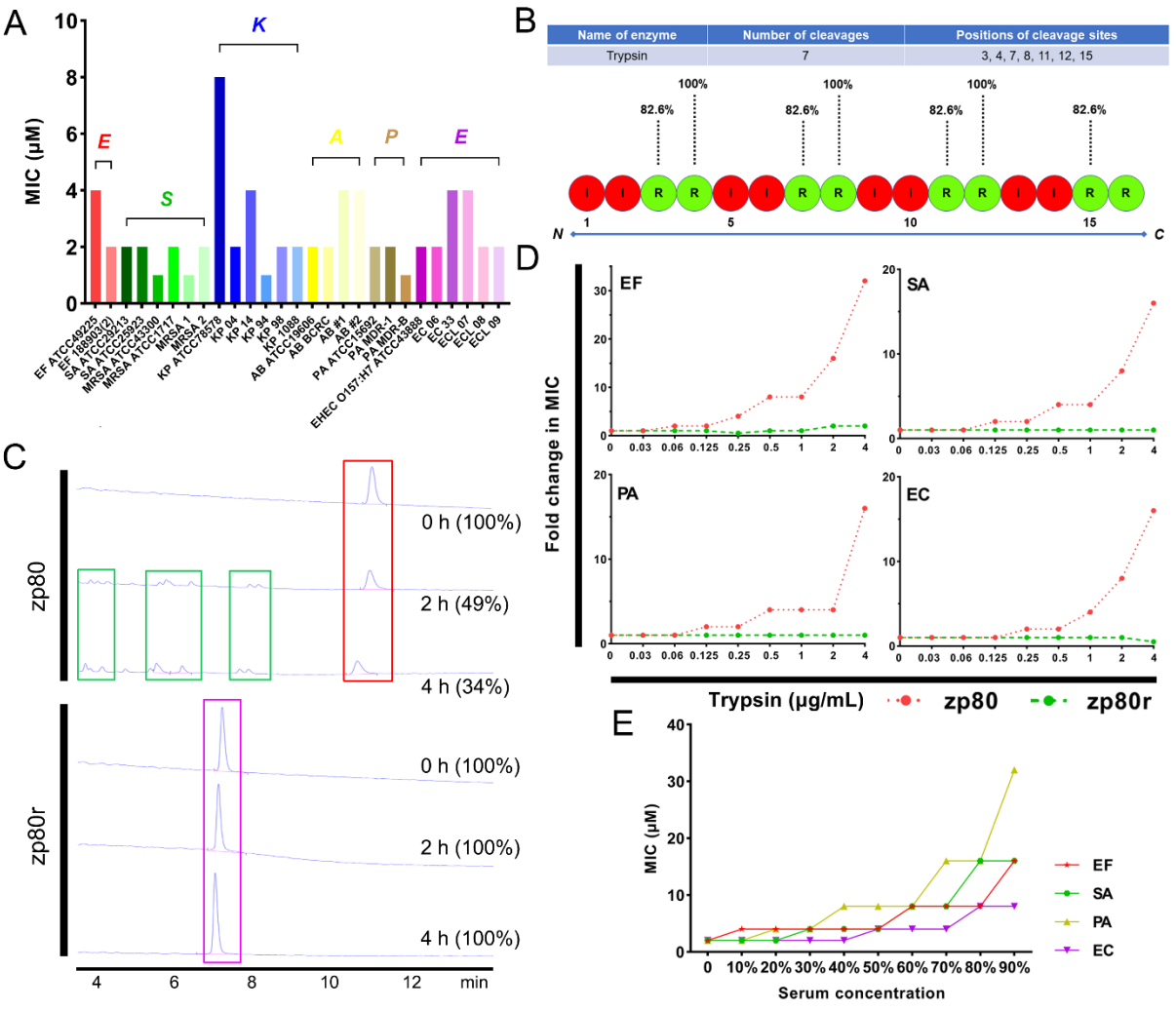

Figure 2. (A) MIC values of **zp80r** against a panel of ESKAPE pathogens; (B) Possible trypsin cleavage sites for **zp80** predicted by Expasy; (C) HPLC chromatograms of **zp80** and **zp80r** before and after 4 μg/mL trypsin treatment. Signals of **zp80** and **zp80r** were highlighted in red and pink boxes respectively. Signals from degradative fragments of **zp80** were highlighted in

green box; (D) Fold change in MIC of **zp80** and **zp80r** against four common foodborne bacteria in the presence of trypsin; (E) MIC change of **zp80r** against four common foodborne bacteria in different serum concentrations.

Peptides consisting of only natural amino acids were often questioned about their proteolytic stability [28]. We first employed an online tool Expasy to analyze possible trypsin cleavage sites for **zp80**. The results shown in **Figure 2B** predicted that L-arginine residues of **zp80** could be in vulnerable positions. At positions 3, 7, 11, and 15, there is an 82.6% probability of being hydrolyzed by trypsin. For residues at positions 4, 8, and 12, this probability increases further to 100%. Modification of amino acid residues at these positions may offer a chance to improve their stability.

Next, we applied HPLC to quantitatively analyze the degradation degree of **zp80** and **zp80r** in the presence of trypsin solution. **Figure 2C** revealed that 2 hours of treatment could degrade more than half of **zp80** molecules. After 4 hours of exposure, only 34% **zp80** was left. On the other hand, **zp80r** is more robust against trypsin treatment as the peptide concentration remains unchanged after 4 hours of incubation. These results suggested that **zp80r** has enhanced proteolytic stability.

Since EF, SA, PA, and EC were widely recognized as representative foodborne pathogens, thereinafter, these four strains (two G+ve and two G−ve) were selected to proceed with further studies. We compared the MIC change of **zp80** and **zp80r** in the presence of trypsin. As illustrated in **Figure 2D**, we concluded that the addition of trypsin would significantly decrease the antibacterial efficiency of **zp80**. MIC values of **zp80** increased 16-fold for SA, PA, EC, and 32-fold for EF when cells were incubated in the presence of 4 μg/mL trypsin. By contrast, the same trypsin concentration didn't exhibit a clear negative effect on **zp80r**'s bioactivity against tested strains. It can be inferred that trypsin leads to the degradation of **zp80** but fails to recognize chirality-modified **zp80r**. This data was consistent with HPLC results, strongly supporting the conclusion that D-arginines substitution enhanced proteolytic stability.

Having verified **zp80r**'s improved stability against trypsin, its antibacterial activity in FBS was evaluated next. Compared with the single trypsin treatment, the serum contains a more complex mixture of enzymes and is closer to the real in-vivo microenvironment. **Figure 2E** indicated that 30% or below serum concentration resulted in an almost negligible effect on the bioactivity of **zp80r** against all tested strains. As the ratio of serum increased, MIC values

began to rise, suggesting that certain components in serum started to interfere with **zp80r**. In 90% serum solution, MIC values of **zp80r** were 8 μM (EC), 16 μM (EF, SA), and 32 μM (PA) respectively, showing a 4 − 16 folds increase compared with the control groups with 0% serum. However, note that 90% serum concentration should be an extremely harsh condition. In such an adverse environment, **zp80r** still maintained modest activity to these foodborne pathogens. Since D-type amino acids exhibited both nutritional and medicinal values in food [29], this substitution highlighted its potential wide application range.

*3.3 Peptide **zp80r**'s working efficiency and low cytotoxicity*

In the process of storage and transportation, food products are sometimes in a state which is not the best fit for bacterial growth, such as nutrient deficiency, low temperature, hypoxia, et al [30]. These unfavorable environments are beneficial for inhibiting bacterial growth on the one hand, while on the other hand, they also pose the risk of inducing persisters [31]. Drug resistance of persisters to antibiotics has strengthened, making it increasingly difficult to control [32]. Here, we found that when normal bacterial cells were subjected to nutritional deprivation for 48 hours, their sensitivities to traditional antibiotics generally decreased markedly (**Figure 3A**). For G+ve strains, EF, and SA, MICs of vancomycin for starvation-induced persisters were both 32 μM, far higher than that for normal bacterial cells of 1 μM and 0.5 μM, respectively. For G−ve strains, MICs of colistin increased from 1 μM to 4 μM (PA) and 0.5 μM to 32 μM (EC). Comparatively, **zp80r** maintained the same level of antibacterial activity in both normal cells and starvation-induced persisters. This may be due to the fact that **zp80r** damaged the cell membrane in a physical attack mode, and it is hard for bacteria to acquire resistance in a short term. Meanwhile, the low temperature didn't cause an obvious influence on both the antibiotic or **zp80r** treatments in this study.

Bacterial cells have strong motility on the food surface, which is conducive to their rapid spread and cross-contamination. Thus, novel compounds that could inhibit bacterial swarming motility are highly desired [33]. We, therefore, investigate the capability of **zp80r** in suppressing cellular swarming behavior. **Figure 3C** showed that the migration distance of four strains inoculated onto a semisolid agar plate containing 10 μM **zp80r** decreased by 20% (EF), 38% (SA), 31% (PA), and 15% (EC). Therefore, the presence of **zp80r** was considered to limit bacterial movement. Furthermore, observed reduced bacterial density after peptide treatment also hinted that **zp80r** could kill some superficial cells which interacted with peptide molecules directly.

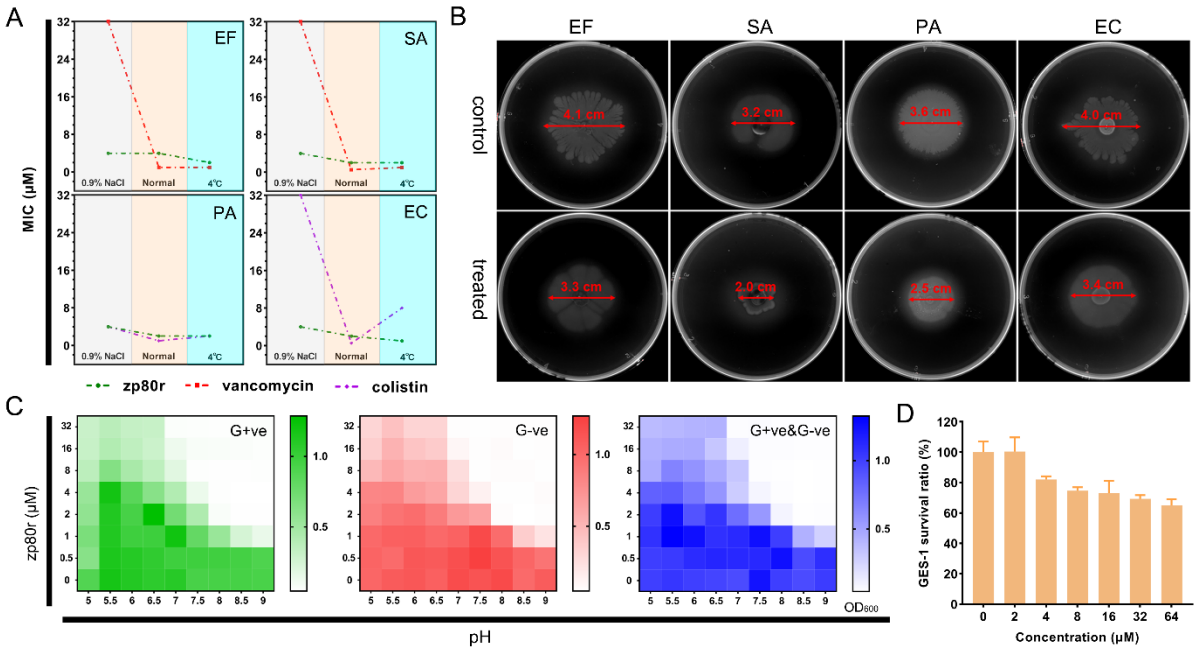

Figure 3. (A) Drug sensitivity of **zp80r** and approved antibiotics against persisters; (B) Swarming motility of four bacteria in the absence or presence of 10 μM **zp80r**. (C) Growth situation of bacteria under varied pH values. The green checkerboard graph represents OD_{600} of two G+ve strains EF and SA mixture after 24 hours of **zp80r** treatment. Similarly, the red graph represents two G−ve strains PA and EC mixture and the blue graph represents the mixture containing all four strains; (D) Cytotoxicity of **zp80r** against GES-1.

pH values sometimes hampered the activity of antimicrobial agents [34]. We sought to assess whether low pH or high pH conditions could inactivate **zp80r**. The pH value of freshly prepared MHB is 7.5. Preliminary experiments confirmed that all four strains were able to proliferate after 24 hours of incubation in the pH range of 5 - 9, though they may not fully grow in some circumstances. From **Figure 3B**, it can be seen that in neutral and basic environments, **zp80r** has favourable antibacterial efficiency against both the G+ve mixture (EF and SA), the G−ve mixture (PA and EC), and the four-strain mixture. These results were consistent with the MIC data. In acidic conditions, the bioactivity of **zp80r** against a pathogenic mixture was slightly weakened. However, even for pH at 5, 8 μM **zp80r** could reduce bacterial proliferation ratio of 58% (G+ve), 51% (G−ve), and 54% (G+ve and G−ve) respectively compared to untreated groups. These data suggested that **zp80r** has a good pH tolerance in killing multiple bacterial species.

Furthermore, the cytotoxicity of **zp80r** was also investigated. The gastrointestinal tract is the core region for food digestion. Therefore, the GES-1 was chosen to preliminarily evaluate **zp80r**'s safety. As shown in **Figure 4C**, the half maximal inhibitory concentration (IC_{50}) of **zp80r** to GES-1 was > 64 μM, which was much higher than its MIC values against ESKAPE bacteria. We proposed that cationic characteristics of **zp80r** may play a key role in this cell selectivity since bacterial membranes usually presented more negative charges in contrast to mammalian normal cell lines [35].

*3.4 Peptide **zp80r** works in a bactericidal mode and causes membrane damage*

From double staining images (**Figure S1**), PA's cell viability before and after **zp80r** treatment can be visualized. In the control group, an overwhelming majority of bacterial cells emitted green fluorescence, and very low red fluorescence was detected, indicating high cell membrane integrity and no damage. While as the treatment concentrations increased gradually from 1 MIC, 2 MIC to 4 MIC, more red signals were captured along with decreased green signals. These pictures demonstrated that bacterial cells have suffered a fatal attack by **zp80r** in a dose-dependent manner.

Time-killing curve (**Figure S2**) further proved that above MIC level, **zp80r** killed ESKAPE strains in the bactericidal mode. Compared to the control group, 4 hours of treatment at 8 MIC could lead to a dramatic reduction of live bacteria (5.8 $\log_{10}$ CFU/mL for EF, 6.5 $\log_{10}$ CFU/mL for SA, 5.6 $\log_{10}$ CFU/mL for PA and 5.8 $\log_{10}$ CFU/mL for EC). Indiscriminate killing efficiencies against various pathogens hinted that **zp80r** could be a promising broad-spectrum antibacterial agent.

SEM was then used to observe the morphological changes after the **zp80r** treatment. Compared to untreated groups, **zp80r**-treated cells exhibited conspicuous deformation (**Figure 4A**). EF showed obvious shrinkage and its surface was less smooth than the control one. Clear dotted pores can be seen on SA and EC. For PA, treated cells had pronounced curly and deformed appearances. These images collectively verified that **zp80r** would incur significant cellular abnormalities.

Next, we sought to visualize possible cell content leakage caused by **zp80r**-induced membrane disruption. GFP-expressing EC is an engineered strain that could emit green light by a biosynthesizing specific fluorescent protein. Cells in the control group were regarded to have intact membrane structure, thus all expressed GFP was harboured within the cytoplasm. Suffering from attack may result in membrane damage, leading to GFP leakage and a

consequent decrease in fluorescence value. As depicted in **Figure 4B**, after 2 hours of incubation with 8 μM **zp80r**, only around 70% GFP signal was captured, indicating that cytoplasm leakage may have taken away some GFP. As to 16 μM and 32 μM groups, the remaining GFP ratio further decreased to less than 60%.

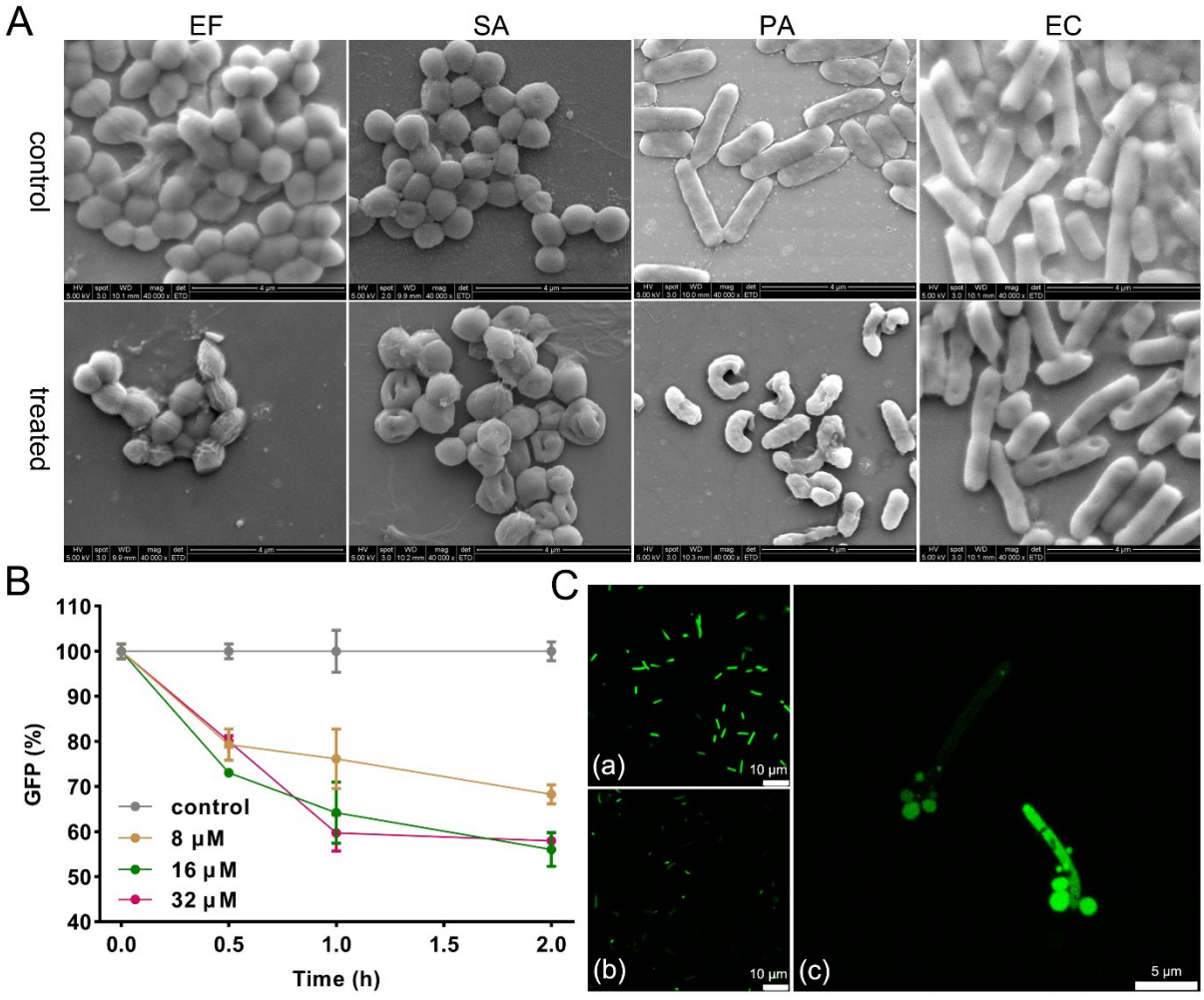

Figure 4. (A) SEM images of bacteria before and after 4 MIC **zp80r** treatment; (B) Green fluorescence leakage ratio after various concentrations of **zp80r** treatment; (C) Confocal images of (a) untreated GFP-expressing EC, (b) treated with 4 MIC **zp80r** and (c) a zoom-in picture of the treated group.

Through confocal pictures, we were able to monitor GFP dissipation intuitively. By comparing **Figure 4C** (a) and (b), dramatic reductions in fluorescence intensity can be detected, reconfirming the rationality of the membrane destruction assumption. In **Figure 4C** (c), we

captured a shot in which GFP was released from two EC cells. These corroborative pieces of evidence supported that **zp80r** would be a membrane-targeting pore former.

*3.5 Peptide **zp80r** triggered ROS and membrane dysfunction*

When bacterial cells are subjected to environmental stress like antibacterial agent treatment, their ROS levels would increase dramatically, leading to severe damage to cell structures [36]. Herein, bacterial ROS accumulation after **zp80r** treatment was measured. **Figure 5A** revealed that **zp80r** upregulated the intracellular oxidative stress of all tested four strains significantly ($p < 0.0001$) even at respective 0.5 MICs. The trend of increasing ROS conformed to the dose-dependent manner, suggesting that **zp80r** may affect the biological function of bacterial cells.

Next, we systematically and quantitatively investigated the degree of damage to bacterial membranes by **zp80r** (**Figure 5B**). G−ve strains have a layer of the outer membrane (OM), which was believed to resist some extraneous chemicals [37]. NPN assay verified that **zp80r** could permeate OM of PA and EC, breaking through the first line of bacterial defense. Moreover, the PI assay demonstrated that **zp80r** was able to further penetrate the whole cytoplasmic membrane system of both G+ve and G−ve bacteria. Their effect was similar to that of the commonly used surfactant Triton X-100.

Meanwhile, membrane potential alteration of EF and SA was monitored by $DiSC_3(5)$. Cells treated with PBS and 5 μM valinomycin were used as negative and positive controls. The results shown in **Figure 5C** indicated that treatments with **zp80r** would cause membrane potential dissipation of EF and SA within seconds. Compared to the well-known membrane potential modulator valinomycin, the process mediated by **zp80r** was more rapid, suggesting that the interaction of **zp80r** molecules with cell membrane could lead to prompt cationic electrical movement across the phospholipid bilayers.

In summary, these mechanistic studies collectively depicted that **zp80r** displayed multiple effects on foodborne pathogens via membrane targeting. After the interaction, it first induced depolarization by dissipating membrane potential. The helical structure was then inserted into the membrane system, leading to membrane damage and subsequently ROS response. These results jointly contributed to membrane dysfunction, envelop integrity deficiency, cellular content leakage, and finally bacterial death.

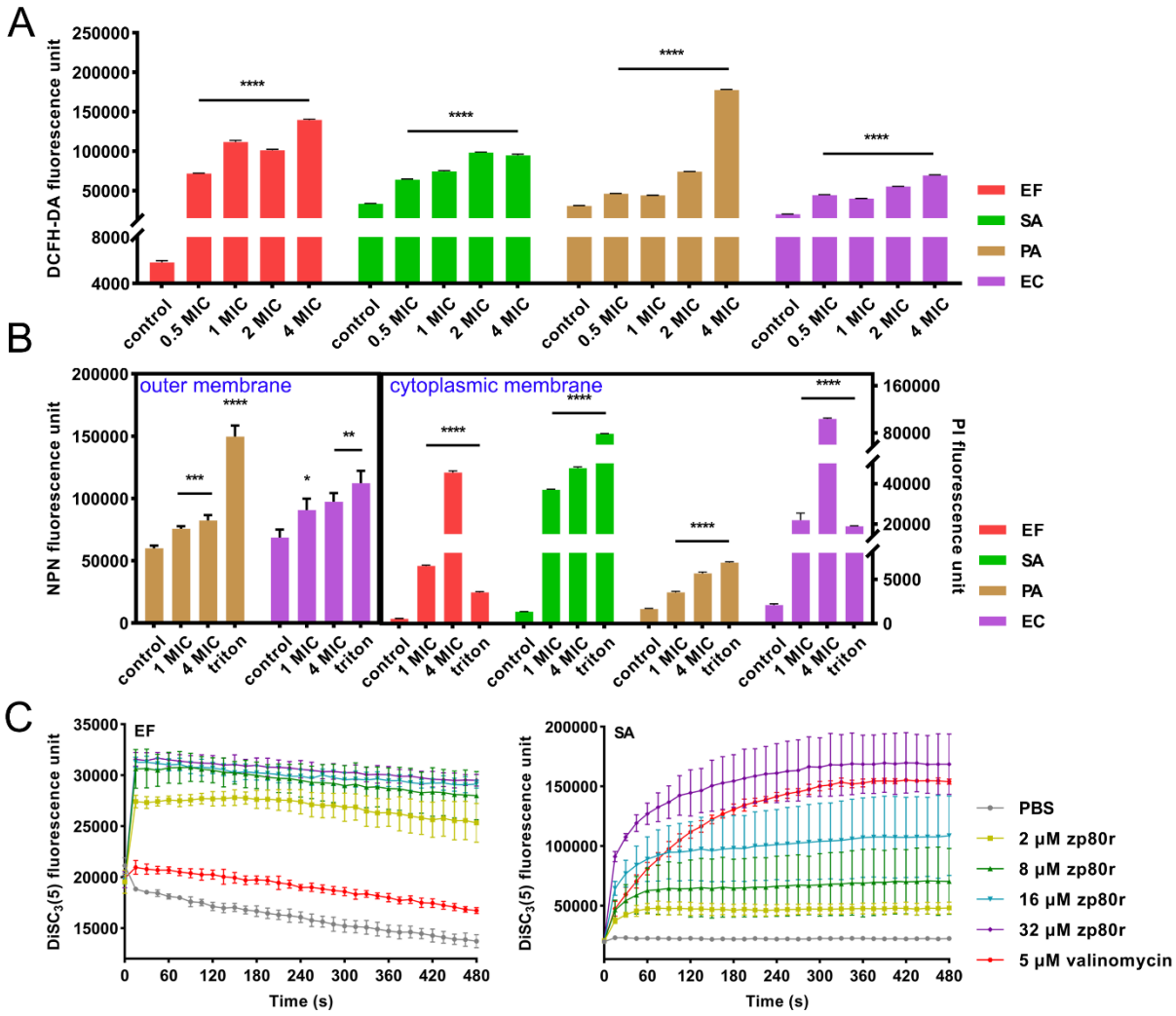

Figure 5. (A) ROS responses of four bacteria after **zp80r** treatment determined by DCFH-DA. ****p < 0.0001; (B) Outer membrane and cytoplasmic membrane permeability tests after **zp80r** treatment by NPN and PI staining respectively. *p < 0.05, **p < 0.01, ***p < 0.001, ****p < 0.0001; (C) Membrane potential alternation after **zp80r** treatment determined by $DiSC_3(5)$.

*3.6 Application of **zp80r** in controlling multiple bacterial contaminations in chilled fresh pork*

Pork is rich in nutrients and water, thus being regarded as an ideal substrate for bacterial reproduction [38]. Low-temperature storage can't effectively kill pathogens. More severely, diversified bacterial communities co-existed in chilled fresh meat, exacerbating the difficulty of food safety control [39]. We, therefore, evaluated the actual application potential of **zp80r** in controlling bacterial growth in retailed pork. A mixture of EF, SA, PA, and EC was applied to contaminate pork pieces. As shown in **Figure 6A**, pre-contaminated pork pieces were treated

with PBS, **zp80r,** and nisin respectively. After 4 days of storage at 4 ℃, the color of the meat began to change significantly. On day 7, the pork piece treated with PBS shrank obviously in comparison with its day 0 and it gave off a strong offensive odor. Furthermore, the texture looked loose and some thick liquid seeped out. This should be attributed to tissue decay and water loss caused by bacterial decomposition. Comparatively, the **zp80r**-treated pork piece emitted a slighter smell and didn't have a lot of exudates.

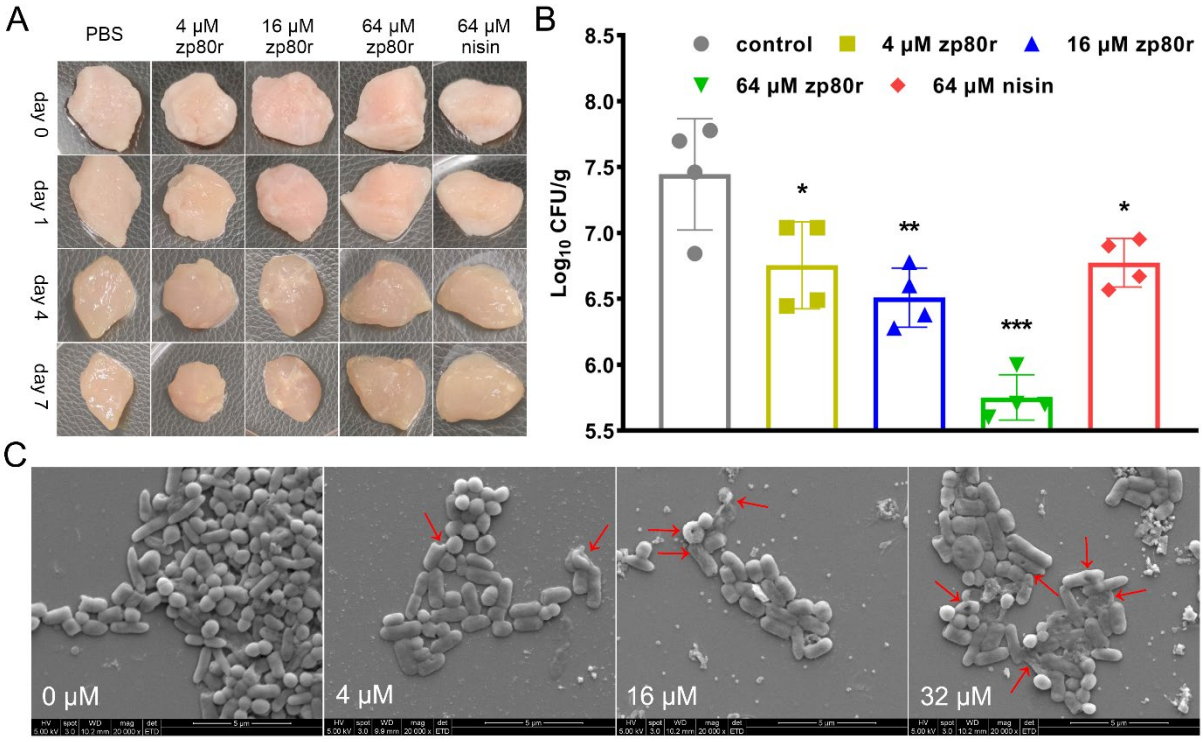

Figure 6. (A) Sensory observation of contaminated pork pieces after varied treatment; (B) Live bacteria count of a total of four strains. *$p < 0.05$, **$p < 0.01$, ***$p < 0.001$; (C) SEM images of **zp80r**-treated multiple bacterial contaminated pork leaching solutions. Deformations of cells were indicated by red arrows.

Live bacterial number was counted thereafter (**Figure 6B**). Compared to the control group, bacterial colonies decreased by 0.69 $\log_{10}$ CFU/g for 4 μM **zp80r** treatment group, 0.95 $\log_{10}$ CFU/g for 16 μM **zp80r** treatment group and 1.70 $\log_{10}$ CFU/g for 64 μM **zp80r** treatment group respectively. By contrast, 64 μM nisin treatment only resulted in 0.68 $\log_{10}$ CFU/g reduction. This showed that even an approved food additive nisin, still performed strugglingly to combat contaminations where G−ve and G+ve strains co-existed.

At last, we observed the morphology of mixed bacteria in untreated or **zp80r**-treated pork leaching solutions (**Figure 6C**). For the untreated group, a variety of normal bacterial forms can be identified, suggesting that different bacterial communities co-existed well in chilled fresh pork. After the **zp80r** treatment, deformative cells were captured. Pores and disintegration can be seen on both rod and spheroid bacteria. To summarize, **zp80r** exhibited favourable antibacterial potential in chilled fresh pork, especially in intractable multiple contamination systems, which was worthy of further research and development.

4. Conclusion

Multiple bacterial co-existence on food product surfaces has put forward higher requirements for its safety control. Here we reported a newly designed peptide **zp80r** with eight D-arginine residues. Introducing this unnatural amino acid significantly improved peptides' proteolytic stability. It showed a broad antibacterial spectrum against all tested ESKAPE pathogens and demonstrated low cytotoxicity to human normal gastric cells. Peptide **zp80r** also exhibited excellent adaptability in killing bacterial cells at unconventional environments like low temperature and basic pH. Mechanistic studies proved that **zp80r** penetrated inside the cytoplasmic membrane, induced membrane potential dissipation, and trigger ROS response. Persisters with increased resistance to traditional antibiotics remained sensitive to **zp80r**. Lastly, **zp80r** performed better at dealing with multiple bacterial contaminations than nisin. These results highlighted that **zp80r** could be a promising candidate for controlling foodborne G+ve and G−ve mixture infection.

Credit authorship contribution statement

Ping Zeng: conceptualization, methodology, formal analysis, investigation, writing - original draft; Pengfei Zhang: methodology, formal analysis, investigation; Lanhua Yi: methodology, formal analysis; Kwok-Yin Wong: resources, supervision, funding acquisition; Sheng Chen: resources, supervision; Kin-Fai Chan: supervision, project administration, funding acquisition; Sharon Shui Yee Leung: resources, writing - review & editing, supervision, project administration, funding acquisition.

Declaration of competing interest

The authors declare no competing financial interest.

Acknowledgments

We are thankful to Prof. Lin Zhang and Dr. Judeng Zeng for providing the GES-1 cell line. We are thankful to Prof. Chris Lai for providing the two EF strains. We are thankful to Dr. Yu Wai Chen for analyzing the 3D structure of peptide **zp80r**. We acknowledge the financial support from the Research Grants Council of Hong Kong (Grant 531 No. C5026-16G) and Health and Medical Research Fund Hong Kong (Grant No. 21200782).

References

[1] M.S. Mulani, E.E. Kamble, S.N. Kumkar, M.S. Tawre, K.R. Pardesi, Emerging Strategies to Combat ESKAPE Pathogens in the Era of Antimicrobial Resistance: A Review, Front Microbiol, 10 (2019) 539.

[2] J.N. Pendleton, S.P. Gorman, B.F. Gilmore, Clinical relevance of the ESKAPE pathogens, Expert Rev Anti Infect Ther, 11 (2013) 297-308.

[3] D.M. De Oliveira, B.M. Forde, T.J. Kidd, P.N. Harris, M.A. Schembri, S.A. Beatson, D.L. Paterson, M.J. Walker, Antimicrobial resistance in ESKAPE pathogens, Clin Microbiol Rev, 33 (2020) e00181-00119.

[4] T.M. Privalsky, A.M. Soohoo, J. Wang, C.T. Walsh, G.D. Wright, E.M. Gordon, N.S. Gray, C. Khosla, Prospects for Antibacterial Discovery and Development, J Am Chem Soc, 143 (2021) 21127-21142.

[5] N. Levy, T. Cravo Oliveira Hashiguchi, M. Cecchini, Food safety policies and their effectiveness to prevent foodborne diseases in catering establishments: A systematic review and meta-analysis, Food Res Int, 156 (2022) 111076.

[6] A. Patil, R. Banerji, P. Kanojiya, S.D. Saroj, Foodborne ESKAPE Biofilms and Antimicrobial Resistance: lessons Learned from Clinical Isolates, Pathog Glob Health, 115 (2021) 339-356.

[7] T. Eklund, Inhibition of growth and uptake processes in bacteria by some chemical food preservatives, J Appl Bacteriol, 48 (1980) 423-432.

[8] J.D. Piper, P.W. Piper, Benzoate and Sorbate Salts: A Systematic Review of the Potential Hazards of These Invaluable Preservatives and the Expanding Spectrum of Clinical Uses for Sodium Benzoate, Compr Rev Food Sci Food Saf, 16 (2017) 868-880.

[9] J. Tkaczewska, Peptides and protein hydrolysates as food preservatives and bioactive components of edible films and coatings - A review, Trends Food Sci Tech, 106 (2020) 298-311.

[10] P. Zeng, L. Yi, Q. Cheng, J. Liu, S. Chen, K.-F. Chan, K.-Y. Wong, An ornithine-rich dodecapeptide with improved proteolytic stability selectively kills gram-negative food-borne

559 pathogens and its action mode on Escherichia coli O157:H7, Int J Food Microbiol, 352
560 (2021) 109281.
561 [11] J. Wang, X. Dou, J. Song, Y. Lyu, X. Zhu, L. Xu, W. Li, A. Shan, Antimicrobial
562 peptides: Promising alternatives in the post feeding antibiotic era, Med Res Rev, 39 (2019)
563 831-859.
564 [12] E. Dell'Olmo, R. Gaglione, M. Sabbah, M. Schibeci, A. Cesaro, R. Di Girolamo, R.
565 Porta, A. Arciello, Host defense peptides identified in human apolipoprotein B as novel food
566 biopreservatives and active coating components, Food Microbiol, 99 (2021) 103804.
567 [13] P. Zeng, Q. Cheng, J. Xu, Q. Xu, Y. Xu, W. Gao, K.-Y. Wong, K.-F. Chan, S. Chen, L.
568 Yi, Membrane-disruptive engineered peptide amphiphiles restrain the proliferation of
569 penicillins and cephalosporins resistant Vibrio alginolyticus and Vibrio parahaemolyticus in
570 instant jellyfish, Food Control, 135 (2022) 108827.
571 [14] L. Yi, P. Zeng, J. Liu, K.-Y. Wong, E.W.-C. Chan, Y. Lin, K.-F. Chan, S. Chen,
572 Antimicrobial peptide zp37 inhibits Escherichia coli O157:H7 in alfalfa sprouts by inflicting
573 damage in cell membrane and binding to DNA, LWT, 146 (2021) 111392.
574 [15] A. Colagiorgi, R. Festa, P.A. Di Ciccio, M. Gogliettino, M. Balestrieri, G. Palmieri, A.
575 Anastasio, A. Ianieri, Rapid biofilm eradication of the antimicrobial peptide 1018-K6 against
576 Staphylococcus aureus: A new potential tool to fight bacterial biofilms, Food Control, 107
577 (2020) 106815.
578 [16] S.H. Toushik, M.F.R. Mizan, M.I. Hossain, S.-D. Ha, Fighting with old foes: The pledge
579 of microbe-derived biological agents to defeat mono- and mixed-bacterial biofilms
580 concerning food industries, Trends Food Sci Tech, 99 (2020) 413-425.
581 [17] L. Yuan, N.I. Wang, F.A. Sadiq, G. He, Interspecies Interactions in Dual-Species
582 Biofilms Formed by Psychrotrophic Bacteria and the Tolerance of Sessile Communities to
583 Disinfectants, J Food Prot, 83 (2020) 951-958.
584 [18] Y.L. Vishweshwaraiah, A. Acharya, V. Hegde, B. Prakash, Rational design of
585 hyperstable antibacterial peptides for food preservation, NPJ Sci Food, 5 (2021) 26.
586 [19] L. Yi, P. Zeng, K.-Y. Wong, K.-F. Chan, S. Chen, Controlling Listeria monocytogenes
587 in ready-to-eat leafy greens by amphipathic α-helix peptide zp80 and its antimicrobial
588 mechanisms, LWT, 152 (2021) 112412.
589 [20] N. Wiradharma, U. Khoe, C.A. Hauser, S.V. Seow, S. Zhang, Y.Y. Yang, Synthetic
590 cationic amphiphilic alpha-helical peptides as antimicrobial agents, Biomaterials, 32 (2011)
591 2204-2212.

[21] S. Singh, H. Singh, A. Tuknait, K. Chaudhary, B. Singh, S. Kumaran, G.P. Raghava, PEPstrMOD: structure prediction of peptides containing natural, non-natural and modified residues, Biol Direct, 10 (2015) 73.
[22] M.A. Wikler, Methods for dilution antimicrobial susceptibility tests for bacteria that grow aerobically: approved standard, CLSI (NCCLS), 26 (2006) M7-A7.
[23] E. Gasteiger, C. Hoogland, A. Gattiker, M.R. Wilkins, R.D. Appel, A. Bairoch, Protein identification and analysis tools on the ExPASy server, The proteomics protocols handbook, (2005) 571-607.
[24] C.J.C. Edwards-Gayle, G. Barrett, S. Roy, V. Castelletto, J. Seitsonen, J. Ruokolainen, I.W. Hamley, Selective Antibacterial Activity and Lipid Membrane Interactions of Arginine-Rich Amphiphilic Peptides, ACS Appl Bio Mater 3(2020) 1165-1175.
[25] Qipeng Cheng, P. Zeng, Hydrophobic-hydrophilic Alternation: An effective Pattern to de novo Designed Antimicrobial Peptides, Curr Pharm Des, (2022).
[26] D. Ciumac, H. Gong, X. Hu, J.R. Lu, Membrane targeting cationic antimicrobial peptides, J Colloid Interface Sci, 537 (2019) 163-185.
[27] T.A.E. Ahmed, R. Hammami, Recent insights into structure-function relationships of antimicrobial peptides, J Food Biochem, 43 (2019) e12546.
[28] Z. Lai, X. Yuan, H. Chen, Y. Zhu, N. Dong, A. Shan, Strategies employed in the design of antimicrobial peptides with enhanced proteolytic stability, Biotechnol Adv, 59 (2022) 107962.
[29] G.L. Marcone, E. Rosini, E. Crespi, L. Pollegioni, D-amino acids in foods, Appl Microbiol Biotechnol, 104 (2020) 555-574.
[30] T. Moretro, S. Langsrud, Residential Bacteria on Surfaces in the Food Industry and Their Implications for Food Safety and Quality, Compr Rev Food Sci Food Saf, 16 (2017) 1022-1041.
[31] X. Xiong, J. Kong, D. Qi, X. Xiong, Y. Liu, X. Cui, Presence, formation, and elimination of foodborne pathogen persisters, JSFA Rep, 2 (2022) 4-16.
[32] M. Wang, E.W.C. Chan, Y. Wan, M.H. Wong, S. Chen, Active maintenance of proton motive force mediates starvation-induced bacterial antibiotic tolerance in Escherichia coli, Commun Biol, 4 (2021) 1068.
[33] S. Rutschlin, T. Bottcher, Inhibitors of Bacterial Swarming Behavior, Chem Eur J, 26 (2020) 964-979.

[34] M.A. Hitchner, L.E. Santiago-Ortiz, M.R. Necelis, D.J. Shirley, T.J. Palmer, K.E. Tarnawsky, T.D. Vaden, G.A. Caputo, Activity and characterization of a pH-sensitive antimicrobial peptide, Biochim Biophys Acta Biomembr, 1861 (2019) 182984.
[35] K.A. Brogden, Antimicrobial peptides: pore formers or metabolic inhibitors in bacteria?, Nat Rev Microbiol, 3 (2005) 238-250.
[36] P. Zeng, L. Yi, M. Wong, S. Chen, K.-F. Chan, K.-Y. Wong, Synthetic Hexadecapeptide Prevents Postharvest Pectobacterium carotovorum (subsp. brasiliensis BC1) Infection via Destabilizing Cell Envelope and Suppressing Biosynthesis of Arginine and Peptidoglycan, ACS Food Sci Technol, 1 (2021) 614-624.
[37] J. Shi, C. Chen, D. Wang, Z. Wang, Y. Liu, The antimicrobial peptide LI14 combats multidrug-resistant bacterial infections, Commun Biol, 5 (2022) 926.
[38] D.-M. Meng, S.-N. Sun, L.-Y. Shi, L. Cheng, Z.-C. Fan, Application of antimicrobial peptide mytichitin-CB in pork preservation during cold storage, Food Control, 125 (2021) 108041.
[39] C. Zhou, J. Wang, R. Li, K. Ye, High-throughput sequencing analysis of the bacterial community for assessing the differences in extraction methods of bacteria separation from chilled pork, LWT, 134 (2020).